Turkish Online Journal of Qualitative Inquiry (TOJQI)
Volume 12, Issue 6, July, 2021: 10192 - 10208

Research Article

Conversion, Simulation, and Engine Testing of a Single Cylinder Port-fuel Injected (PFI) Atkinson Cycle Engine Based on an Otto Cycle Engine

Jose Luis L. Villalon

MAPUA UNIVERSITY
School of Graduate Studies
jllvillalon@mymail.mapua.edu.ph

Abstract

Downsized ICEs have been widely used for various applications worldwide. One of the feasible methods in improving engine efficiency and consumption is applying an Atkinson cycle engine. This research aimed to convert a single-cylinder Otto cycle engine that will accomplish an Atkinson cycle effect by modifying the intake cam timing and compression ratio. A wheel dynamometer was built to analyze the engine's baseline performance and behavior. The engine modification underwent a two-part CFD-1D simulation with a GA optimization strategy to obtain baseline performance and design improvements. It was found that the engine modification with the optimized fuel mapping significantly reduced the average BSFC by 36.07% at 3000rpm range, 8.58% decrease at 5000rpm range, and 14.9% decrease at 8000rpm range. The corresponding engine power resulted in a 68.93% increase at the 3000rpm range, 1.76% decrease at the 5000rpm range, and 3.49% decrease at the 8000rpm range.

Keywords:

1. Introduction

In 1882, a British engineer named James Atkinson introduced the Atkinson Cycle Engine (ACE). The principle behind this was to derive the Otto cycle by increasing the expansion stroke relative to the compression stroke through a variable piston displacement. The engine consists of complex linkages wherein the ER is greater than the CR, which gives more thermal efficiency than the Otto cycle. Furthermore, the development of ACEs was long halted since the over-expansion effect was difficult to achieve at that time. Other literature works refer to the Atkinson process as the Sargent cycle.

One of the modern approaches in achieving the Atkinson cycle is modifying the intake cam timings rather than the piston movement. This particular method uses a manually adjusted cam profile to attain the desired performance at a specific operating range. This strategy has two variations: Late Intake Valve Closing (LIVC) and early intake valve closing. A strategy involving the LIVC cam phasing may reduce the fuel consumption by 15g/kWh.

The performance of the Atkinson cycle, with variable piston movement, promises higher efficiency than the Otto Cycle Engine (OCE) because it can operate at a higher Compression Ratio (CR) without the occurrence knocking[1]. On the other hand, the power and torque of an ACE, with the LIVC approach, is lower than that of the OCE, especially in the low load condition[1], because the Atkinson cycle permits lower CRs the manual LIVC.

1.1 Statement of the Problem

The Philippines' continuous economic improvement has policies that mitigate the following factors: environmental, equitable, and economic methods. The urban transportation emissions in Metro Manila, as an example, contributes to 65% of the nationwide air pollution. High poverty rates hamper the modernization of public transportation as most commuters prefer the cheapest form available without sustainability. Simultaneously, the government's push in modernizing jeepneys and tricycles is rendered non-equitable to operators.

1.2 Objective of the Study

This research aims to convert a naturally aspirated single-cylinder spark-ignition engine from Otto cycle into Atkinson cycle, with minimal modifications, to improve fuel economy without huge compromise to engine performance. The objectives are summarized accordingly: (1) Firstly, create a baseline engine performance test thru an engine dynamometer using the Otto cycle engine. (2) Secondly, create an engine model that will simulate the baseline engine using Converge CFD and GT-Power coupling, then utilize it upon conversion to Atkinson cycle engine. (3) Thirdly, determine the optimum compression ratio and LIVC design for the Atkinson cycle engine using the Genetic Algorithm (GA). (4) Fourth, perform an actual engine performance test thru a dynamometer for the Atkinson cycle engine. (5) Lastly, optimize the fuel mapping of the EFI for the Atkinson cycle engine to further reduce the fuel consumption.

1.3 Scope

This study's scope is primarily focused on establishing theoretical simulations and verifying them through actual tests in modifying an OCE into ACE. The engine modifications' focus is changing the cam timings and CR (i.e., changing the piston top profile) to minimize the complex conversion and maximize the overall fluid dynamic effects. The engine design and improvement will disregard part-load operations and only focus on three specific engine speed ranges: 3000rpm, 5000rpm, and 8000rpm. The simulation will rely on two-part software, namely GT-Power and Converge CFDTM. Converge will simulate the in-cylinder fluid effects such as swirl ratio, tumble ratio, and turbulence energy. At the same time, GT-Power software will provide a 1D simulation of the engine output based on Converge's data. A comparison between the theoretical data and actual wheel dynamometer tests became the basis of implementing the ACE.

2. Review Of Related Works

Expansion to Higher Efficiency – Investigation of the Atkinson Cycle in small Combustion Engines (Pertl et al., 2012)

Pertl et al. found that large displacement engines have higher efficiencies than smaller displacement engines, and one option is to reduce the Compression to Expansion Ratio (CER). There are numerous potential for downsized engine development, especially in PTWs. Research shows that the annual mass production of PTWs reached 88 million worldwide, and the demand will rise 7% annually from 2012 to 2015. Research also suggests that the use of PTWs will significantly impact total fuel savings and CO2 mitigations, considering that typical consumers have an average of 1.3 occupants per vehicle. Thus, the development of small engines is essential. The objective was to improve reciprocating piston heat engines with various CERs. Results indicate that the ACE's thermal efficiency was 6% higher than the baseline engine and the efficiency at WOT had an acceptable result within a specified speed range. The range of efficiencies was determined using a 1-dimensional simulation from the actual engine dyno tests. Finally, a typical PTW engine's intake valve timing was compared to an ACE with CER of 0.5 while at WOT scenarios.

Investigations of Atkinson Cycle Converted from Conventional Otto Cycle Gasoline Engine (Feng et al., 2016)

Feng et al. demonstrated a calculation to determine the optimum clearance volume of an OCE converted into ACE. The concept is based on determining the volume power, as seen in Equation 1, of the baseline engine, henceforth the OCE.

$$P_L = \frac{P_e}{cV_s} \quad (1)$$

Where $P_L, P_e, V_s,$ and c denote the volume power in KWL, max engine power in KW, Otto cycle displacement in L, and the number of cylinders, respectively. Then, to mitigate the effects of knocking, it was assumed that the ACE volume power must be similar in proportion to the baseline engine. Thus, the formula in Equation 2 is shown below.

$$cV_s' = \frac{P_e'}{P_L} \quad (2)$$

$P_e{}'$, and $V_s{}'$ is denoted as the target engine power in KW, and the effective Atkinson cycle displacement in L, respectively. Finally, finding the effective displacement of the Atkinson cycle will lead to finding its respective clearance volume, as seen in Equation 3.

$$CR = \frac{V_s{}' + V_{AC}{}'}{V_{AC}{}'} \tag{3}$$

Where CR, and $V_{AC}{}'$ denote the Atkinson compression ratio and the Atkinson clearance volume, respectively. According to Feng et al., the CR for both baseline and Atkinson engines are equal in proportion since the priority of the design is to mitigate knocking.

Simulation of Intake and Exhaust Valve Timing on Internal Combustion Engine (Dahlan et al., 2017)

The design of experiments (DOE) is also an optimization option used in the design of ICEs. The GT-Power software can perform the DOE and view the post-process results. A 1.6L VVT Proton Iriz engine was experimented with to achieve a Miller cycle approach and reduce fuel consumption. The primary objective was to determine the optimum valve timings at different engine speeds to obtain less fuel consumption using the GT-Power software. The overall results showed positive results in BSFC but the minimal effect in applying the Miller cycle concept due to the dramatic decrease of compression ratio and engine performance[5]. Furthermore, the Proton Iriz engine lacked a forced induction system commonly found in engines operating a Miller cycle concept.

An Introduction to Genetic Algorithms (Carr, J. 2014)

The GA is applied in numerical problems that require an optimal solution by prioritizing or disregarding a particular function. Research in evolutionary computation is where genetic algorithms represent, in which by simulating the concept of biological reproduction and natural selection to providing the “fittest” solutions. Furthermore, they are also very effective in solving problems even with a lack of information, compared to random search or other high-demanding algorithms.

3. Methodology

The research methodology was strategically implemented in four phases. The first phase focused on setting up the baseline data of the Otto cycle engine. The next phase was designing and simulating the modifications for the ACE. Next, fabrication of the engine components was the third phase. Lastly, the final dynamometer tests and optimization of the fuel mapping was performed.

3.1 Phase 1: Obtaining Baseline Data for the Original Engine

This research's first phase was to conduct a baseline engine test via wheel dynamometer and determine the following engine parameters: brake power, brake torque, and BSFC. Then, a coupled simulation was performed using Converge CFD™ and GT-Power that will produce the same actual engine performance results. It should be noted that Converge will handle the in-cylinder CFD simulation, and then this data will be sent to GT-Power to calculate the theoretical engine performance. The baseline parameters are shown in Table 3.0.

Table 3.0 Engine specifications by actual measurement.

Specification	Measurement
Displacement	125 cc
Bore	52.4 mm
Stroke	57.9 mm
Geometric comp. ratio	9.5:1
Conrod length	93.5 mm
Piston pin diameter	13 mm

Converge is a state-of-the-art computational fluid dynamics (CFD) software efficient in the runtime calculation because it is primarily designed to generate mesh where complex geometries are present. Converge can produce accurate simulation results using its reliable, detailed chemistry solver and meshing features in a Reynolds-Averaged Navier-Stokes (RANS) modeling approach. Meanwhile, GT-POWER is an automotive tool that was utilized to simulate and predict the performance of the research engine[9].

Building the Dynamometer

The researcher built a wheel dynamometer to conduct a baseline engine performance test. This dynamometer uses an Arduino microcontroller to handle multiple sensor inputs. Simultaneously, a data encoding software named SimpleDyno utilized the sensor inputs to calculate and display the needed output parameters: brake power, brake torque, and BSFC. SimpleDyno is open-source, and it can be programmed based on your sensor's compatibility.

The Arduino senses the roller rpm and engine rpm signals, while SimpleDyno calculates the power and torque based on the roller's inertia. Furthermore, an Accurate Lambda Meter (ALM) monitors the air-fuel ratio (AFR) in the dynamometer.

3.2 Phase 2: ACE Design and Simulation

The second phase of this research was to determine the target parameters for modifying the baseline engine. The target parameters listed in Table 3.1 were computed using the volume power method provided by Feng et al. After that, the intake valve timing and compression ratio were optimized using the Genetic Algorithm.

Table 3.1 Target specifications for the Atkinson cycle engine

Parameter	Target
Effective Displacement	110 cc
Brake Power	8.3 Hp @ 8000 rpm
Effective Compression Stroke	51mm
Effective Compression Ratio	9.5
Geometric Compression Ratio	10.63
CER	0.89

3.3 Phase 3: Fabrication of Engine Parts

The intake cam lobe was fabricated via cam refacing, which follows the desired LIVC from the GA optimization results. Meanwhile a blank piston was fed through a lathe machine to acquire a dome shape pattern, and then it was fed through a milling machine to fabricate the valve pockets. The piston profile was reassured to match with the desired Atkinson engine clearance volume of 13cc, including the valve pockets positioning to avoid collision with the valves.

3.4 Phase 4: Comparison with reference plant

The final research phase was to perform the final engine dynamometer test for the modified engine. The main objective was to further reduce fuel consumption by optimizing the EFI fuel mapping. The optimization of the fuel mapping was possible through a standalone fully programmable Electronic Control Unit (ECU).

3.5 Theoretical Framework

The ICEs have come a long way since they were invented that allowed humans to travel faster and reach further distances with engines' development as they become more efficient. It is undeniable that the further use of ICEs may come to a critical point with the limited source of fossil fuels. Alternative energy supplies are still impractical in terms of cost and supply. Meanwhile, the sudden boost of electric cars in the global market was very sellable to consumers even though EVs are still limited in energy storage, travel range, recharging time, and material costs. There must have a transition from ICE to full electric for the development of such technology, hence the hybrid propulsion systems. In the transition from ICE to fully electric vehicles, the ICE will eventually become obsolete. Hybrid power plants have huge contribution to in bridging the technological gap. Toyota Motor Corp was able to develop a hybrid power plant reaching a thermal efficiency of 18%; whereas Honda was also able to implement their own ACE thru the novel variable valve timing and electronic control, obtaining a lowest BSFC at 220 g/kWh. Another feasible approach is to reuse conventional Otto cycle engines and convert them into Atkinson cycle engines and establish a smoother transition between the two technologies.

3.6 Conceptual Framework

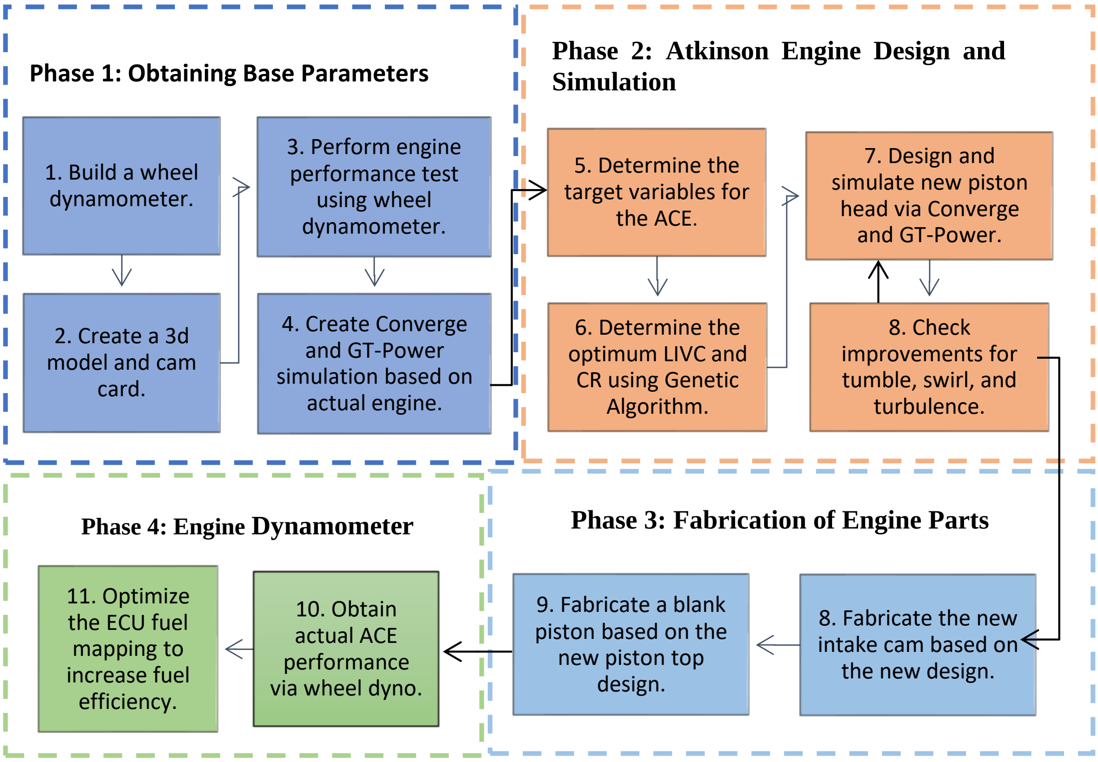

Figure 3.0 Conceptual framework for the design, simulation, and testing of the engine.

4. Results and Discussion

CFD Baseline Simulation

Converge was able to perform the adaptive mesh refinement (AMR), as seen in Figure 4.0. It was estimated that there were more than 800,000 cells during the in-cylinder combustion phase, as depicted in Figure 3.0b, while there were at least 55,000 cells when the piston is at BDC. This case proves that the AMR prioritized the critical fluid mixing phenomena by reducing cell sizing while increasing cell sizing in non-critical events.

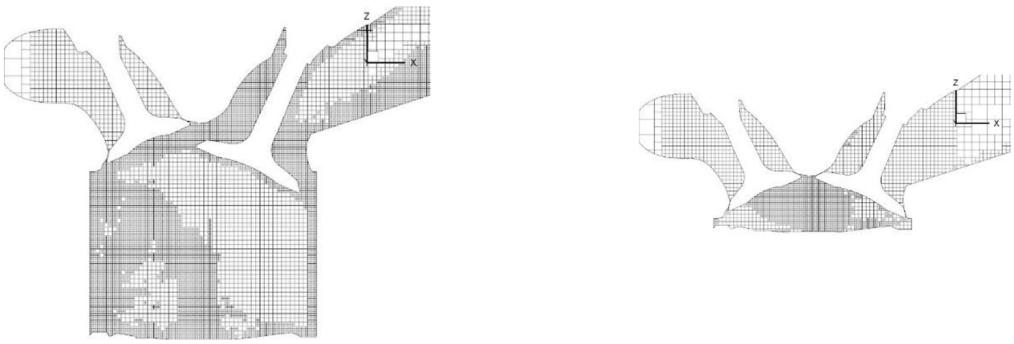

(a) Intake stroke at 450 CA˚

(b) Power stroke at 720 CA˚

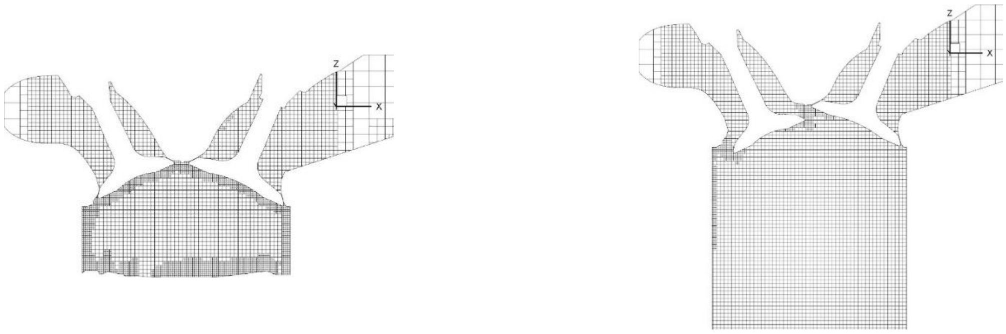

(c) Power stroke at 770 CA˚ (d) Exhaust stroke at 930 CA˚

Figure 4.0 Cross-sectional mesh with AMR.

The three parameters observed in the baseline Converge simulation, namely: tumble ratio, turbulence energy, and swirl ratio, were tested at different engine speeds, as seen in figures 4.1, 4.2, and 4.3. Each scenario started at 350 CA˚ which is during the intake stroke or air-fuel premixing stage. It was observed that the tumble ratio had a slight variation in all specified engine speeds while the swirl ratios and turbulence energies broadly vary in similar engine scenarios. Moreover, the tumble and swirl ratios slightly decrease with increasing engine speed, while the turbulence energy slightly increases, respectively. It should be noted that the swirl ratio in figure 4.12 is accepted to have a negative quantity due to the direction of the angular velocity of the flow (Richards and Senecal 2019).

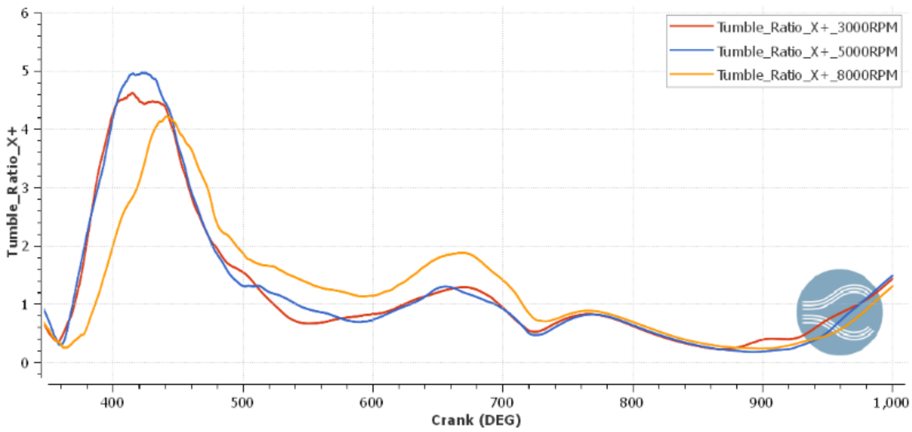

Figure 4.1 Tumble ratio of baseline engine at 3000, 5000, and 8000 rpm.

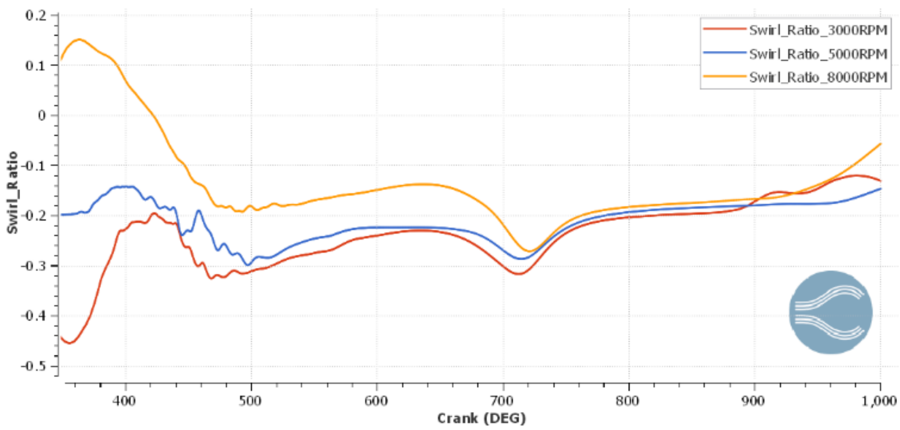

Figure 4.2 Swirl ratio of baseline engine at 3000, 5000, and 8000 rpm.

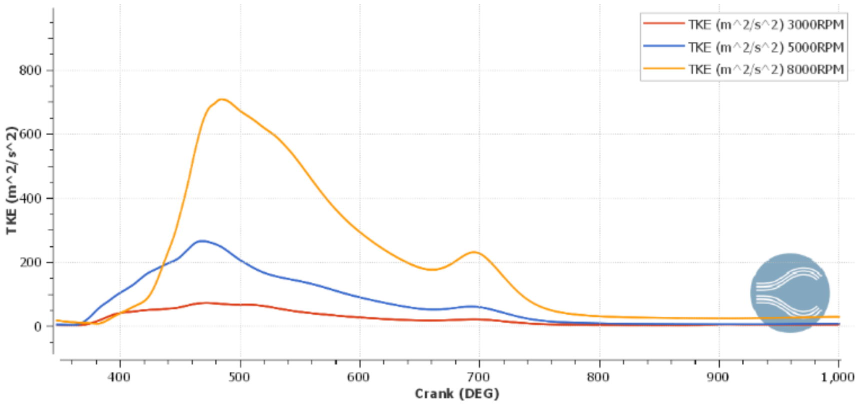

Figure 4.3 Turbulence kinetic energy of baseline engine at 3000, 5000, and 8000 rpm.

The post results were processed using Tecplot, which depicts one of the engine speed scenarios shown in Figure 4.4. Tecplot can render animations by displaying the fluid domain in Euler-Lagrangian form, contours, or gradients. Therefore, the gasses' tumble ratio, swirl ratio, and turbulence kinetic energy were visually observed according to the respective engine setup. Increased tumble ratio, swirl ratio, and turbulence kinetic energy result in better combustion, which constitutes faster flame propagation. The flame propagation can be observed using the temperature contours during the combustion stroke, as depicted in Figure 4.4.

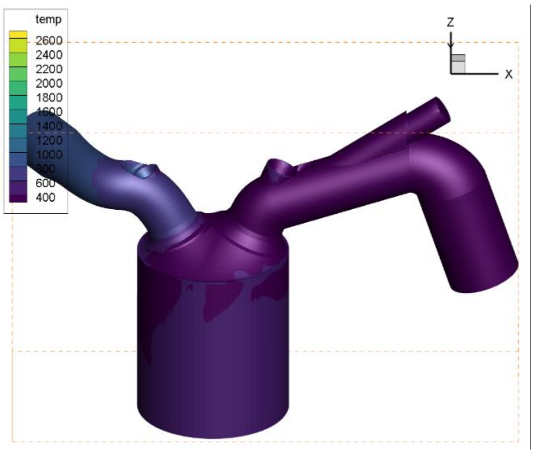

(a) Intake Stroke BDC datum at 0 CA˚

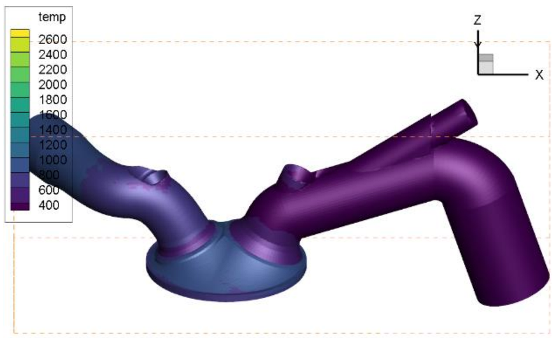

(b) TDCI after intake at 180 CA˚

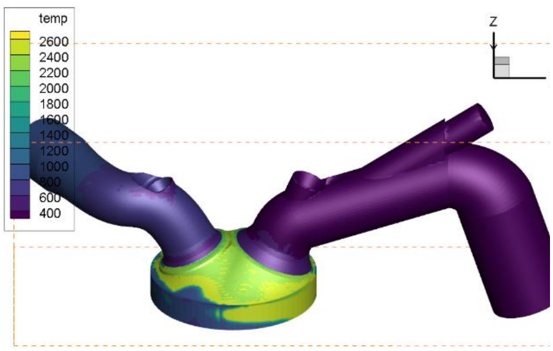

(c) Spark ignition phase at 210 CA˚

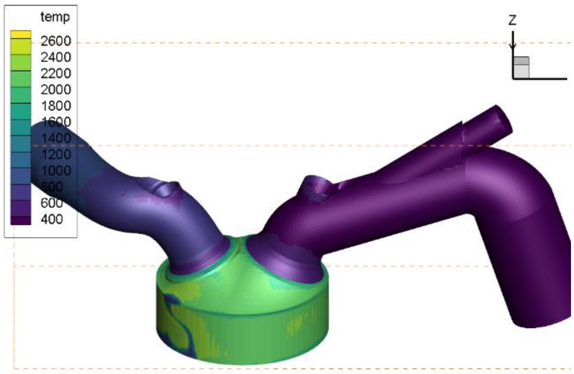

(d) Flame propagation at 230 CA˚

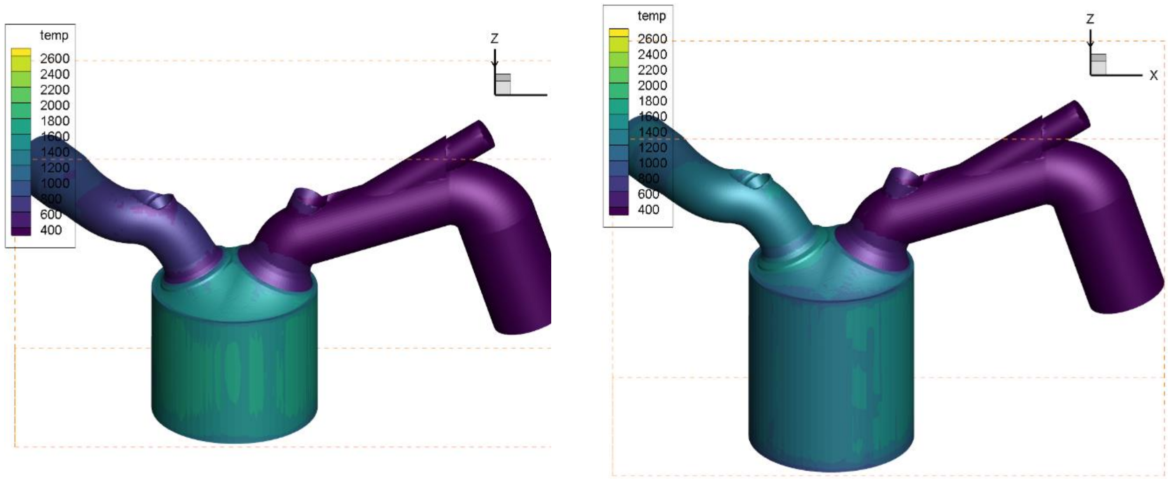

(e) Expansion stroke at 270 CA˚ (f) Expansion BDC at 360 CA˚

Figure 4.4 Post-processing using Tecplot, with temperature contours.

Baseline Engine Performance

Figure 4.5 shows the maximum power and torque at their respective engine speeds, plotted using GT-POST, a post-processing software by GT-POWER. The baseline data also covered three engine speed scenarios, mainly 3000rpm, 5000rpm, and 8000rpm, with power output values at 3.88Hp, 6.30Hp, and 10.27Hp, and torque values at 9.20Nm, 9.3Nm, and 9.13Nm, respectively. The scenarios in these tests assumed that the engine was operating at WOT, and the engine speeds were static.

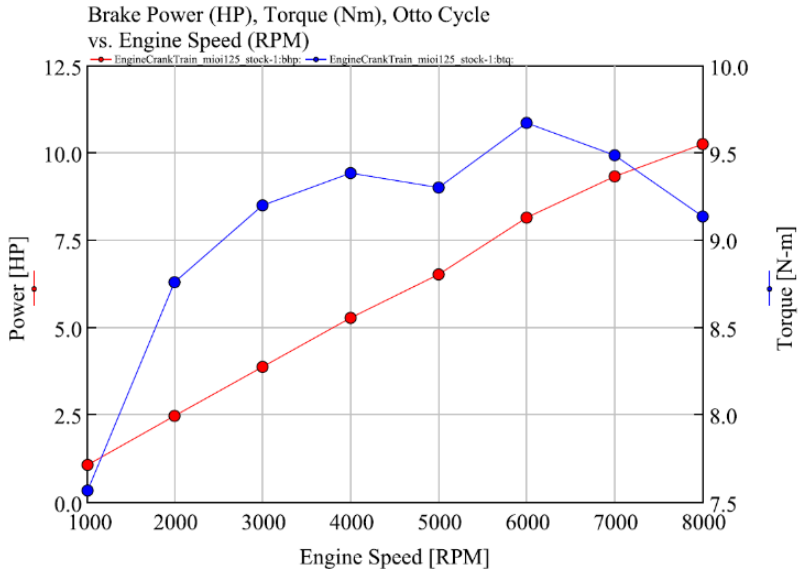

Figure 4.5 Baseline power and torque data via GT-Post.

The baseline dynamometer tests for the low operating range in Figure 4.6 achieved a max wheel power of 3.22HP at 3594rpm and a max wheel torque of 6.55Nm at 3386rpm. The engine power and torque were calculated using the overall ratio from the instantaneous roller rpm (RPM1) and engine rpm (RPM2) with their respective peak curves, which resulted in 1.16HP at 3594rpm and 1.94Nm at 3386rpm. A similar strategy was also performed for the 5000rpm and 8000rpm tests with the average results listed in Table 1.2.

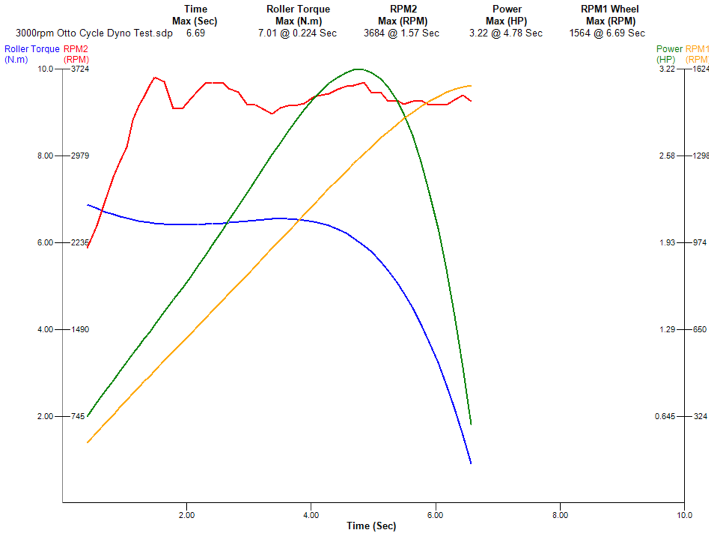

Figure 4.6 Baseline power and torque data via GT-Post.

The accuracy of the simulation in comparison to the actual engine test is displayed in Table 4.1. The percent errors of the GT power vs. engine dyno results at the 3000rpm range were 70.01% and 78.91% in power and torque results, respectively. Furthermore, the inaccuracy was caused by the partial engagement of the centrifugal clutch in the secondary pulley, which was proven by monitoring the roller rotational speed relative to the engine rotational speed. Additionally, the respective power and torque percent errors on the 5000rpm range were 10.32% and 36.13%, which were considerably lower than the low-speed range due to the fully engaged CVT. Furthermore, the power and torque percent errors from the 8000rpm range were 17.14% and 7.01%, respectively. The latter was performed at WOT, and the CVT was fully engaged during the test, reflecting a more accurate performance than the 3000rpm dyno test. The engine model was used to modify the ACE since the 5000rpm and 8000rpm tests achieved low percent errors.

Table 4.1 Accuracy of wheel dyno vs GT-Power in baseline engine test.

Engine Speed (RPM)	GT-Power		Wheel Dynamometer		Percent Error	
	Power (Hp)	Torque (Nm)	Ave. Power (Hp)	Ave. Torque (Nm)	Power (Hp)	Torque (Nm)
3000	3.88	9.20	1.16	1.94	70.01%	78.91%
5000	6.30	9.3	6.95	5.94	10.32%	36.13%
8000	10.27	9.13	12.03	8.49	17.14%	7.01%

Optimization of LIVC

The prediction accuracy of using the BSFC as a target variable in attaining LIVC timing was very low because the LIVC strategy was not achieved in the simulation trials. The GA solutions always arrive at achieving EIVC as an optimum solution; thus, the Atkinson displacement was used as a target variable. Simultaneously, the cam angle multiplier was set as an independent variable, and the cam lift multiplier was set as a sweep variable. The settings mean that the independent variable will have different optimum designs for each case, while the sweep variable will have an optimum design for all cases. It should also be noted that the genetic algorithm still used the baseline engine parameters as initial values, and the algorithm itself will calculate the adjustments based on the target values and assigned ranges. The GA results for the optimizing LIVC are shown in Figure 4.7.

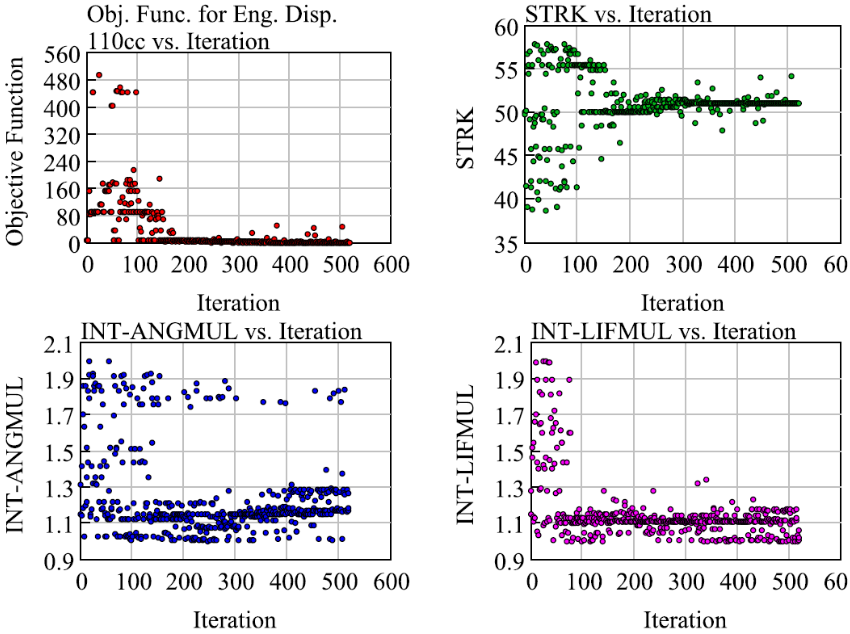

Figure 4.7 Optimization of LIVC timing via genetic algorithm.

Preliminary test results showed that the objective function reached convergence, indicating that the intake cam parameters (angle multiplier, lift multiplier) and engine stoke attained an optimum design. The three solutions for the angle multiplier were solved for each case, but one solution was chosen for the LIVC design. Moreover, the stroke and cam data were used to test the power output, which produced 8.65919 Hp, an acceptable deviation compared to the computed target of 8.3 Hp. The preliminary results also showed that the simulated BSFCs were higher at each RPM than the baseline engine.

Optimization of CR

Another optimization session was performed using the effective compression ratio as the independent variable and the BSFC as the target variable, as depicted in Figure 4.8. Furthermore, the cam data from the preliminary test were adapted for this simulation, and the baseline engine geometries were retained as well. The new data showed that the GCR' was valued at 11:1, which is higher than the computed value of 10.63. The simulation also indicated that the BSFC values were lower than the baseline engine at all engine speed ranges. In contrast, the volumetric efficiency was higher due to the lack of input data in the intake manifold assembly. Nonetheless, the GCR' of 11:1 was used for the piston modification.

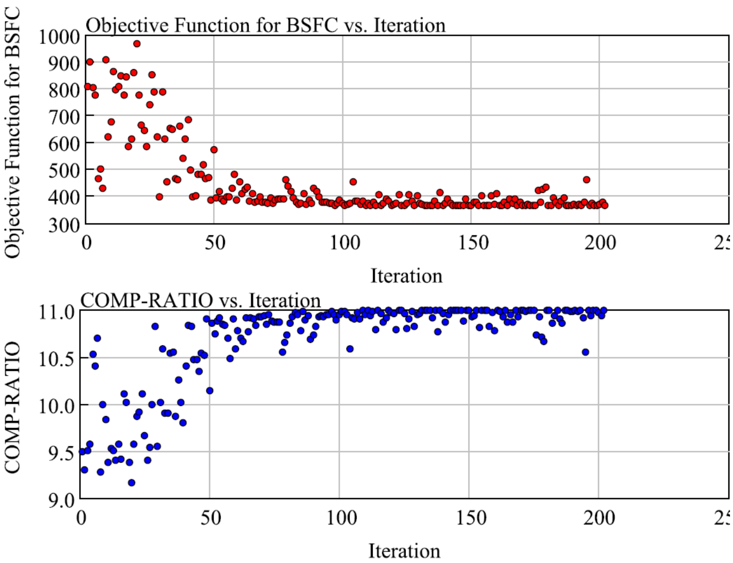

Figure 4.8 Optimization of compression ratio via genetic algorithm.

Optimum Cam Profile for ACE

As seen in Figure 4.9, the adjusted cam profiles were used to reference the LIVC approach based on the preliminary GT-Power simulation. The new cam lifts were interpolated using GT-Power and matched the corresponding values with the baseline crank angle values. The updated cam card was used as a reference for modifying the camshaft, wherein the intake valve closing was delayed by 40 CA˚, while the maximum valve lift was increased by 0.4mm.

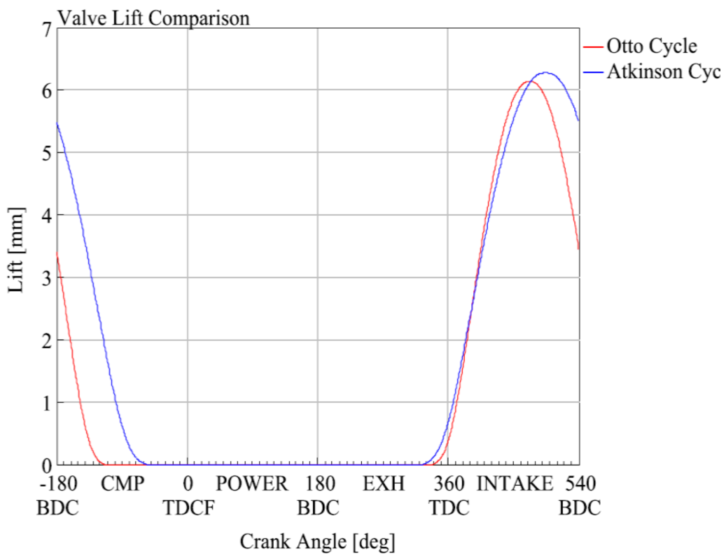

Figure 4.9 Cam Lifts of Otto and Atkinson cycle.

CFD Modified Engine Simulation

The new cam timings and piston design were applied in the Converge case setup for the Atkinson cycle CFD simulation. The CFD results are shown in Figure 4.10, 4.11, and 4.12, which illustrates the tumble ratio, swirl ratio, and turbulent kinetic energy between the baseline and modified engines at 8000rpm. The graphs also start at 350 CA˚ during the TDC intake stroke. The tumble ratio, swirl ratio, and turbulence energy dictate the quality of air-fuel mixing, resulting in better combustion while mitigating the effects of engine knocking (Feng, et al. 2016).

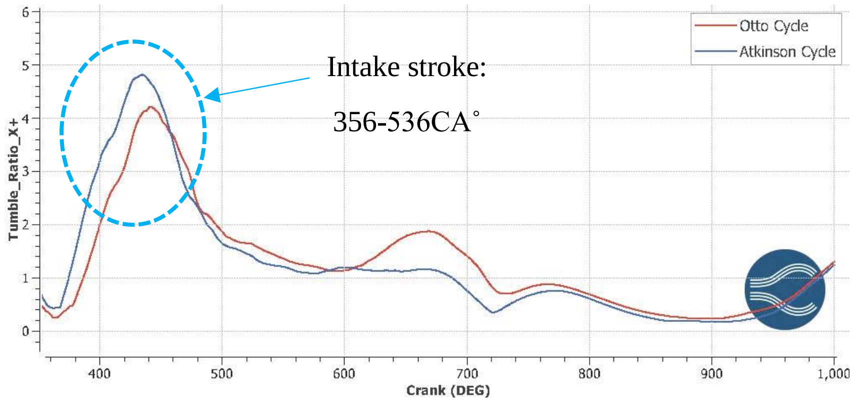

Figure 4.10 Tumble ratio comparison between Otto cycle and Atkinson cycle.

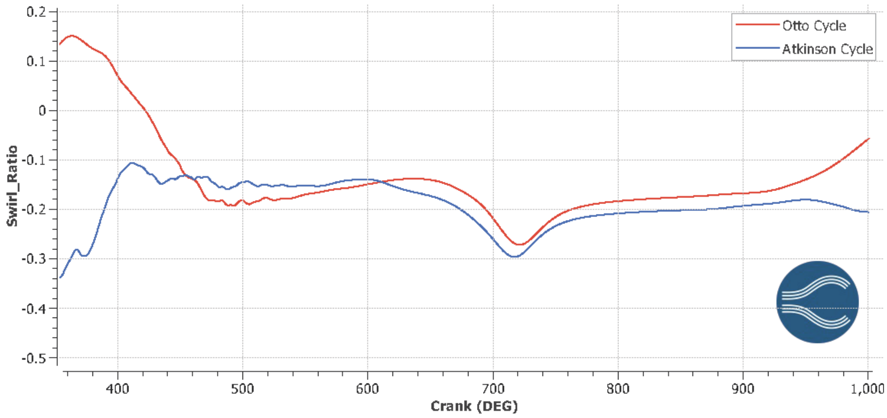

Figure 4.11 Swirl ratio comparison between Otto cycle and Atkinson cycle.

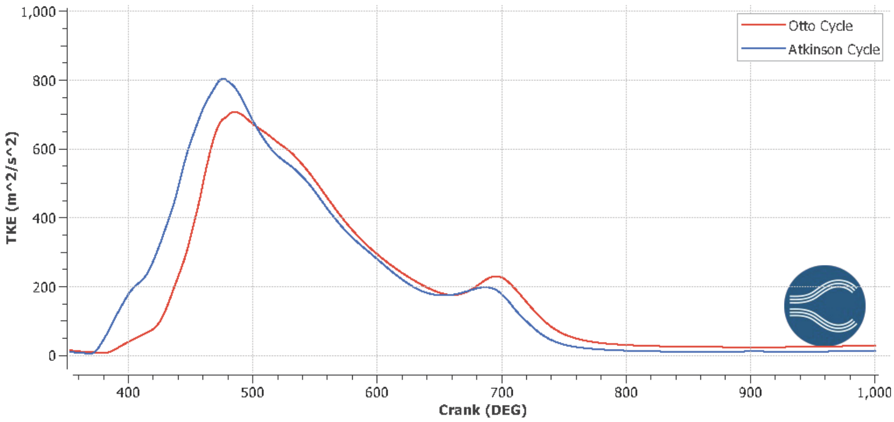

Figure 4.12 Turbulent kinetic energy comparison between Otto cycle and Atkinson cycle.

The results showed improvements in tumble ratio, swirl ratio, and turbulence energy for the Atkinson cycle CFD simulation. The negative result from the swirl ratio dictates a different direction of angular velocity from the fluid flow, which is an acceptable value. Therefore, the modeled piston modification was used for the actual ACE.

Performance of the ACE

The following engine performance from the GT-Power simulation produced power values at 2.03Hp at 3000rpm, 3.85Hp at 5000rpm, and 7.01Hp at 8000rpm, respectively. Then the torque values were at 4.82Nm, 5.48Nm, and 6.24Nm, respectively. As seen in figure 4.13, this simulation showed a decrease in power and torque compared to the Otto cycle simulation. This case is due to the over-expansion strategy as expected from the previous calculations.

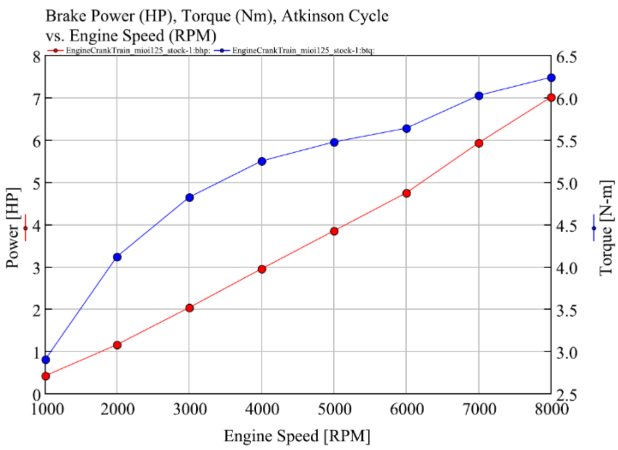

Figure 4.13 Atkinson power and torque data via GT-Post.

The accuracy of actual wheel dynamometer tests compared to the GT-Power simulation for the ACE is shown in table 4.2. The modification of the piston and camshafts while retaining the baseline fuel mapping showed the expected decrease in engine performance as predicted by the GT-Power simulation. The accuracy of the data in the 5000rpm to 8000rpm range proved the effectiveness of GT-Power in predicting the engine performance.

Table 4.2 Accuracy of wheel dyno vs. GT-Power in ACE test.

Engine Speed (RPM)	GT-Power Simulation		Wheel Dynamometer Test		Percent Error	
	Power (Hp)	Torque (Nm)	Ave. Power (Hp)	Ave. Torque (Nm)	Power (Hp)	Torque (Nm)
3000	2.03	4.82	0.52	1.65	74.38%	65.77%
5000	3.85	5.48	4.39	4.81	14.03%	12.23%
8000	7.01	6.24	8.30	7.30	18.40%	16.99%

The percent errors at 3000rpm range resulted at 74.38% and 65.77% for the power and torque, respectively due to CVT transmission losses. Meanwhile, the 5000rpm range tests had percent errors of 14.03% and 12.23% for the power and torque, respectively. Furthermore, the power and torque errors for the 8000rpm range were calculated at 18.40% and 16.99%, respectively. The results also prove higher accuracy than the low-speed test due to the lower percent errors and decreased transmission losses from the CVT. A decrease in engine performance was also observed compared to the baseline test at 8000rpm, mainly due to the overexpansion effect.

Optimization of Fuel Mapping

A final engine test was performed by optimizing the fuel mapping for the ACE to maximize fuel efficiency with minimal performance losses. The brake power comparison of the baseline vs. modified engines resulted to a 68.93% increase at the 3000rpm range, 1.76% decrease at the 5000rpm range, and 3.49% decrease at the 8000rpm range. However, the BSFC comparisons resulted to a 36.07% decrease at 3000rpm range, 8.58% decrease at 5000rpm range, and 14.9% decrease at 8000rpm range. This shows that the optimum BSFC with respect to engine speed is achievable in the 5000rpm range.

The decrease of BSFC while increasing brake power at 3000rpm range in this tests was highly unintuitive but accepted values. One of the main reasons is that the ACE test attempts had higher throttling to reach the 3000rpm range compared to the test attempts in the baseline engine. Furthermore, the throttling is first induced to accelerate the engine from idle up to a specific operating range. At the same time, the fuel demand becomes higher in order to maintain stoichiometric AFR and overcome rotational inertia. Then, the throttling is gradually reduced to maintain that specific speed range, while the fuel map behavior will drastically reduce the fuel demand to maintain the 14.7 AFR. With this in mind, the fuel injection rate of the modified engine was increased at a higher throttling position to effectively accelerate the engine from idle up to 3000rpm, thus generating higher power output and higher torque than the baseline engine. Meanwhile, the reduced effective compression volume of the ACE allowed a considerably low fuel injection rate with 14.7AFR at a lower throttling position to maintain the 3000rpm range, thus achieving lower BSFC than the baseline engine (Ge, Chen and Sun 2010).

Notably, the results obtained in the 3000rpm for this test were still relevant even with the accounted transmission losses because the adequate acceleration from idle up to 3000rpm without engine stalling relies on the fuel map settings. Furthermore, there were experienced cases that the engine will stall if the fuel map settings in 3000rpm and below were not optimized. It was observed that the optimization of the fuel mapping provided a significant advantage in improving fuel economy without the excessive decline in brake power and brake torque. The comparison of the brake power, brake torque, and BSFC between the baseline and modified engine is shown in Figures 4.14, 4.15, and 4.16.

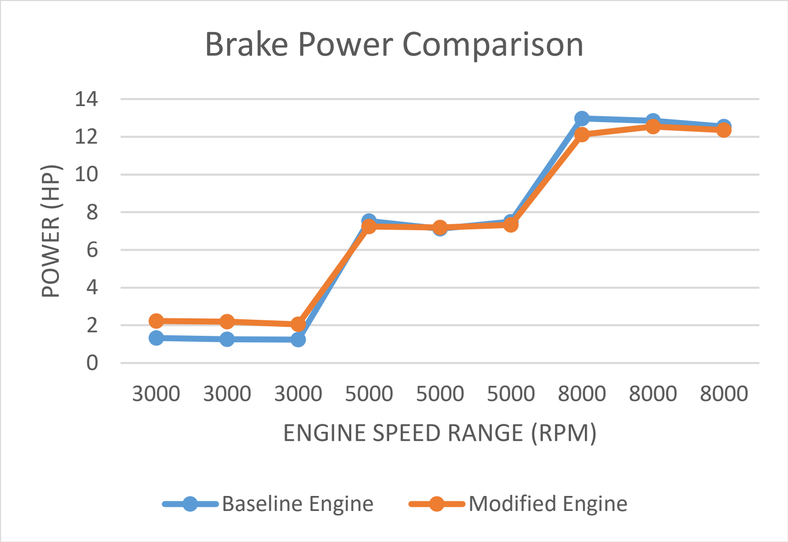

Figure 4.14 Brake power comparison for baseline and modified engine.

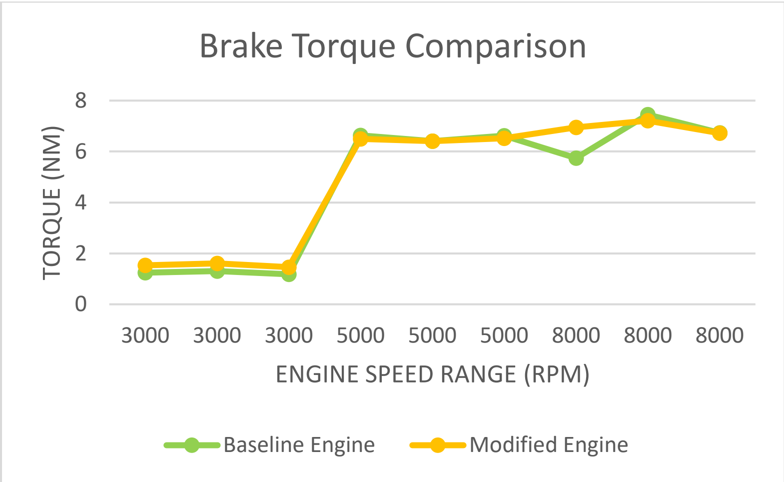

Figure 4.15 Brake torque comparison for baseline and modified engine.

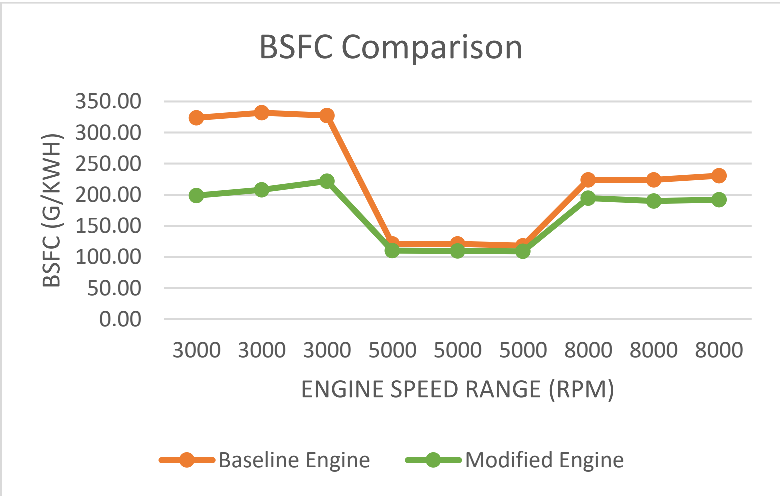

Figure 4.16 BSFC comparison for baseline and modified engine.

5. Conclusion

The conversion, simulation, and engine testing of a single cylinder ACE converted from an OCE were successfully implemented.

1. Firstly, the baseline engine performance was successfully determined by building and utilizing a wheel dynamometer.
2. Secondly, an engine model was successfully created based on the baseline engine performance and was fully utilized for the design modifications.
3. Thirdly, the GA was able to calculate the optimum LIVC and CR for the engine modification. Both parameters were advantageous according to the simulation results, such as improved tumble, swirl, and turbulence energy.
4. Fourth, the wheel dynamometer tests produced by the ACE confirm the engine behavior produced by the simulation results, such as decreased brake power, decreased brake torque, and improved BSFC.
5. Lastly, the BSFC of the modified engine was further improved by optimizing the fuel map with the use of a programmable ECU. It was found that the optimum operating range was 5000rpm since the BSFC was lowest in this operating range, averaging at 109.71g/kWh. To be specific, the BSFC was reduced by 8.58%, while the engine power resulted in a 1.76% decrease at the 5000rpm range.

6. Recommendation

The improvement of this research will support the development of single-cylinder internal combustion engines in the Philippines. Several key areas should improve the implementation of dynamometer tests in this research.

Firstly, the engine crankcase should be separated from the transmission assembly and directly driven to the engine dyno; Thus, the brake engine performance is accurately measured without mechanical losses.

Then, the microcontroller and engine RPM's adequate shielding is vital to prevent noise in the data during tests; with this in mind, the circuit development should also consider incorporating additional sensors.

Next, SimpleDyno is open-source software that uses Visual Basic syntax. The source code improvement of SimpleDyno should contain the proper calibration of sensors into the software. The software should also include the actual BSFC mapping; this will further enhance the internal combustion engines' development, particularly in increasing fuel efficiency and GHG emissions.

Lastly, this research recommends that the additional variable valve timing mechanism to the camshaft will provide extra power to specific engine speed ranges. The methodologies discussed in this research are also pertinent in modifying multiple-cylinder engines from the Otto cycle into the Atkinson cycle.

References

[1] Battistoni, M., Mariani, F., Risi, F., Poggiani, C. (2015). "Combustion CFD modeling of a spark ignited optical access engine fueled with gasoline and ethanol". Journal of Energy Procedia. 82, 424-431. https://doi.org/10.1016/j.egypro.2015.11.829

[2] Crisostomo, N. (2013). The Philippine Jeepney's Black Carbon Emissions: Sustainability Challenges and Solutions. Urban Studies 165: Sustainable Transportation, Individual Essay. https://www.mdpi.com/2071-1050/12/23/10043/pdf

[3] Carr, J. (2014). An introduction to genetic algorithms. Whitman University

[4] Chen, L., Linm J., Sun, F., Wu, C. (1998). "Efficiency of an Atkinson engine at maximum power density". Journal of Energy Conversion Management. 39 (3-4): 337-341. https://doi.org/10.1016/S0196-8904(96)00195-1

[5] Cunningham, D. (2014). SimpleDyno Manual v3.0

[6] Dahlan, A. A., Shahrafi, M., Said, M. F. (2017). "Simulation of intake and exhaust valve timing on internal combustion engine". Automotive Development Center, Faculty of Mechanical Enigneering, Universiti Teknologi Malaysia. 79 (4-7). https://doi.org/ 10.11113/jt.v79.12264

[7] Dingelstadt, R., Fraser, N., Hoffman, H., Taylor, J. "Benefits of late inlet valve timing strategies afforded through the use of intake cam in cam applied to a gasoline turbocharged downsized engine", SAE Technical Paper, 2011-01-0360, 2011, 6-8. https://doi.org/10.4271/2011-01-0360.

[8] Ebrahimi, R. (2011). "Effects of mean piston speed, equivalence ratio and cylinder wall temperature on performance of an Atkinson engine". Journal of Mathematical and Computer Modelling. 53 (5-6): 1289-1297. https://doi.org/10.1016/j.mcm.2010.12.015

[9] Feng, F., Yangtao, Li., Yang, J., Fu, J., Zhang, D., Zheng, G., "Investigations of Atkinson cycle converted from conventional otto cycle gasoline engine", SAE Technical Paper 2016-01-0680, 2016, 2-8. https://doi.org/10.4271/2016-01-0680.

[10] Gamma Technologies (2015). GT-Suite Flow Theory Manual version 2016

[11] Ge, Y., Chen, L., Sun, F. (2010). "Finite time thermodynamic modelling and analysis for an irreversible Atkinson cycle". Journal of Automotive Engineering, 222 (5): 887-894. https://doi.org/10.1243/09544070JAUTO695

[12] Hou, S. (2006). "Comparison of performances of air standard Atkinson and otto cycles with heat transfer considerations". Journal of Energy Conversion and Management. 48 (5): 1683-1690. https://doi.org/10.1016/j.enconman.2006.11.001

[13] Pertl, P., Trattner, A., Abis, A., Schmidt, S., Kirchberger, R., "Expansion to higher efficiency – Investigation of the Atkinson cycle in small combustion engines", SAE Technical Paper 2012-32-0059, 2012, 2-7. https://doi.org/10.4271.2012-32-0059.

[14] Richards, K. J., Senecal, P. K., and Pomraning, E., CONVERGE 2.4, Convergent Science, WI (2019).

[15] Richards, K. J., Senecal. P. K., and Pomraning, E., CONVERGE 2.4 Manual, Convergent Science, WI (2019).

[16] Senecal, P. K., Pomraning, E., Richards, K. J., Briggs, T. E., Choi, C. Y., McDavid, R. M., Patterson, M. A., "Multi-dimensional modeling of direct-injection diesel spray liquid length and flame lift-off length using CFD and parallel detailed chemistry", SAE Technical Paper 2003-01-1043, 2003, https://doi.org/10.4271/2003-01-1043.

[17] Takahashi, D., Koichi N., Yasushi, Y., Yukinori, O., Hiroyuki, N., "Combustion development to achieve engine thermal efficiency of 40% for hybrid vehicles", SAE Technical Paper 2015-01-1254, 2015. https://doi.org/10.4271/2015-01-1254.

[18] Wang, C., Daniel, R., Xu, H., "Research of the Atkinson cycle in the spark ignition engine", SAE Technical Paper 2012-01-0390, 2012, 1-9. https://doi.org/10.4271/2012-01-039.

[19] Zhao, J., Xu M., Li M., Wang, B., Liu, S. (2011). "Design and optimization of an atkinson cycle engine with artificial neural network method". Journal of Applied Energy, 92: 492-502. https://doi.org/10.1016/j.apenergy.2011.11.060

[20] Zhao, J. (2016). "Research and application of over-expansion cycle (Atkinson and miller) engines – a review". Journal of Applied Energy, 185 (1): 303-310. https://doi.org/10.1016/j.apenergy.2016.10.063

[21] Zhao, J., Li, Y., & Xu, F. (2017). "The effects of the engine design and operation parameters on the performance of an Atkinson engine considering heat-transfer, friction, combustion efficiency and variable specific-heat". Journal of Energy Conversion and Management, 151 (1): 16-20.

[22] Yi, J (2010). "Design and optimization of gasoline direct injection engines using computational fluid dynamics". Journal of Advanced direct injection combustion engine technologies and development. Gasoline and gas engines, 166-198. https://doi.org/10.1533/9781845697327.166

[23] Yonekawa, A., Ueno, M., Watanabe, O., Ishikawa, N., "Development of new gasoline engine for accord plug-in hybrid", SAE Technical Paper, 2013-01-1738, 2013, https://doi.org/10.4271/2013-01-1738.

[24] Zhao, Jinxing. 2016. "Research and application of over-expansion cycle (Atkinson and Miller) engines - a review." *Applied Energy* (Elsevier) (185): 300-319.

[25] Hou, S. 2006. "Comparison of Performances of Air Standard Atkinson and Otto Cycles with Heat Transfer Considerations." *Energy Conversion and Management* 1683-1690.

[26] Chen, L., Linm, J., Sun, F., Wu, C. 1998. "Efficiency of an Atkinson Engine at Maximum Power Density." *Energy Conversion and Management* 337-341.

[27] Zhao, Jinxing. 2016. "Research and application of over-expansion cycle (Atkinson and Miller) engines - a review." *Applied Energy* (Elsevier) (185): 300-319.

[28] Dingelstadt, R., Fraser, N., Hoffman, H., Taylor, J. 2011. "Benefits of Late Inlet Valve Timing Strategies afforded through the Use of Intake Cam Applied to a Gasoline Turbocharged Downsized Engine." *SAE Technical Paper 2011-01-0360* 6-8.

[29] Feng, F, Li. Yangtao, J. Yang, J, Fu, D, Zhang, and G. Zheng. 2016. "Investigations of Atkinson Cycle Converted from Conventional Otto Cycle Gasoline Engine." *SAE Technical Paper* (2016-01-0680).

[30] Crisostomo, N. 2013. "The Philippine Jeepney's Black Carbon Emissions: Sustainability Challenges and Solution. Urban Studies 165: Sustainable Transportation, Individual Essay."

[31] Pertl, P., Trattner, A., Abis, A., Schmidt, S., Kirchberger, R.,. 2012. "Expansion to Higher Efficiency - Investigation of the Atkinson Cycle in Small Combustion Engines." *SAE Technical Paper 2012-32-0059* 2-7.

[32] Dahlan, Afiq A, Mohamad Shahrafi, and Mohd F. S. Said. 2017. "Simulation of Intake and Exhaust Valve Timing on Internal Combustion Engine." *Jurnal Teknologi* (79): 47-52.

[33] Gamma Technologies. 2015. *GT-Suite Flow Theory Manual version 2016.* Illinois, USA: Gamma Technologies.

[34] Dahlan, Afiq A, Mohamad Shahrafi, and Mohd F. S. Said. 2017. "Simulation of Intake and Exhaust Valve Timing on Internal Combustion Engine." *Jurnal Teknologi* (79): 47-52.

[35] Carr, Jenna. 2014. *An Introduction to Genetic Algorithms.* Whitman College.

[36] Richards, K. J., and P. K., and Pomaraning, E. Senecal. 2019. *CONVERGE 2.4.* Madison, WI: Convergent Science.

[37] Cunningham, Damien. 2014. *SimpleDyno Manual v3.0*

[38] Zhao, Jinxing. 2016. "Research and application of over-expansion cycle (Atkinson and Miller) engines - a review." *Applied Energy* (Elsevier) (185): 300-319.

[39] Zhao, Jinxing. 2016. "Research and application of over-expansion cycle (Atkinson and Miller) engines - a review." *Applied Energy* (Elsevier) (185): 300-319.

[40] Zhao, Jinxing. 2016. "Research and application of over-expansion cycle (Atkinson and Miller) engines - a review." *Applied Energy* (Elsevier) (185): 300-319.

[41] Feng, F, Li. Yangtao, J. Yang, J, Fu, D, Zhang, and G. Zheng. 2016. "Investigations of Atkinson Cycle Converted from Conventional Otto Cycle Gasoline Engine." *SAE Technical Paper* (2016-01-0680).

[42] Takahashi, D., Koichi N., Yasushi, Y., Yukinori, O., Hiroyuki, N. 2015. "Combustion Development to Achieve Engine Thermal Efficiency of 40% for Hybrid Vehicles." *SAE Technical Paper 2015-01-1254.*

[43] Yonekawa, A., Ueno, M., Watanabe, O., Ishikawa, N. 2013. "Development of New Gasoline Engine for Accord Plug-in Hybrid." *SAE Technical Paper 2013-01-1738.*

[44] Feng, F, Li. Yangtao, J. Yang, J, Fu, D, Zhang, and G. Zheng. 2016. "Investigations of Atkinson Cycle Converted from Conventional Otto Cycle Gasoline Engine." *SAE Technical Paper* (2016-01-0680).

[45] Senecal, P.K., E. Pomraning, K.J. Richards, T.E. Briggs, C.Y. Choi, R.M. McDavid, and M.A. Patterson. 2003. "Multi-Dimensional Modeling of Direct-Injection Diesel Spray Liquid and Flame Lift-off Length using CFD a Parallel Detailed Chemistry." *SAE Technical Paper Series.*